Biophysical Properties and Thermal Stability of Oligonucleotides of RNA Containing 7,8-Dihydro-8-hydroxyadenosine

Ana M. Chauca-Diaz, Yu Jung Choi, Marino J. E. Resendiz
Department of Chemistry, University of Colorado Denver, Science Building, 1151 Arapahoe St, Denver, CO 80204

Received 20 September 2014; revised 22 October 2014; accepted 22 October 2014
Published online 1 November 2014 in Wiley Online Library (wileyonlinelibrary.com). DOI 10.1002/bip.22579

ABSTRACT:

Circular dichroism (CD) was used to assess the stabilization/destabilization imposed by oxidative lesion 7,8-dihydro-8-hydroxyadenosine (8-oxoA) on strands of RNA with different structural motifs. RNA:RNA homoduplex destabilization was observed in a position dependent manner using 10-mers as models that displayed differences between 12.7 and 15.1°C. We found that increasing the number of modifications resulted in depressed T_m values of about 12–15°C per lesion. The same effect was observed on RNA:DNA heteroduplex samples. We also tested the effects of this lesion in short hairpins containing the tetraloop UUCX (X = A, 8-oxoA). We found that the stem was hypersensitive to substitution of A by 8-oxoA and that it destabilized the structure by >23°C. Concomitant substitution at the stem and loop prevented formation of this secondary structure or lead to other less-stable hairpins. Incorporation of this lesion at the first base of the loop had no effect on either structure. Overall, we found that the effects of 8-oxoA on RNA structure are position dependent and that its stabilization may vary from sharp decreases to small increments, in some cases, leading to the formation of other more/less stable structures. These structural changes may have larger biological implications, particularly if the oxidatively modified RNA persists, thus leading to changes in RNA reactivity and function. © 2014 Wiley Periodicals, Inc. Biopolymers 103: 167–174, 2015.

Keywords: nucleic acid stability; 8-oxoadenosine; circular dichroism; oxidative damage of RNA; RNA structural changes

This article was originally published online as an accepted preprint. The "Published Online" date corresponds to the preprint version. You can request a copy of any preprints from the past two calendar years by emailing the Biopolymers editorial office at biopolymers@wiley.com.

INTRODUCTION

Oxidative damage to nucleic acids is an important phenomenon occurring from endogenous and exogenous sources[1–4] and is of relevance in the biogenesis of disease including different cancers and neurological disorders.[5–7] Much of the emphasis regarding reactions between reactive oxygen species (ROS) and nucleic acids has been placed on DNA, due in part, to the potential deleterious effects resulting in mutations and genetic damage.[8] Oxidation of RNA has not been as studied; however, this phenomenon is increasingly attracting interest and has been suggested to play a role in the development of disease.[9–11] Amongst the canonical bases, guanosine and adenosine have the lowest oxidation potentials, 1.29 and 1.42 eV, respectively,[12,13] and are common targets for their corresponding reactions with ROS (e.g., O_2^{2-}, •OH, •OOH, and $^1O_2$). One of the main products arising from these events corresponds to oxidation at the C-8 position to yield the 7,8-dihydro-8-hydroxy-purines, namely

Additional Supporting Information may be found in the online version of this article.

Ana M. Chauca-Diaz and Yu Jung Choi contributed equally to this work
Correspondence to: Marino Resendiz; e-mail: marino.resendiz@ucdenver.edu

Contract grant sponsor: CU Denver and a Faculty Development Grant (to M. J. E. R.)
Contract grant sponsor: University of Colorado Cancer Center (NMR Facilities)
Contract grant number: P30CA046934

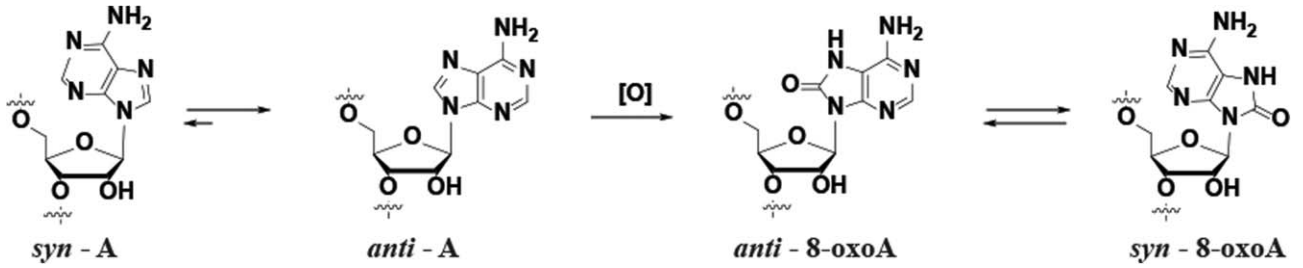

SCHEME 1 Oxidation of the C8-position in adenosine changes the equilibrium between the syn- and anti-conformations.

8-oxo-guanosine and 8-oxo-adenosine (8-oxoA, Scheme 1).[14,15] In fact, these oxidative lesions (1:0.4 ratio 8-oxoG/8-oxoA) constitute about 64% of the main modifications observed in DNA of mammalian chromatin subjected to γ-radiolysis.[16] In this study, we are reporting on the biophysical properties of monomers and oligonucleotides of RNA containing the adenosine adduct 8-oxoA. This lesion has been detected previously in both DNA[17] and RNA.[18] Studies on monomers of this lesion have shown that a conformational change around the glycosidic bond, anti→syn (Scheme 1, right), occurs upon oxidation of adenosine at the C8-position, while equilibrium in adenosine favors the anti-conformation. This change is responsible for the formation of base pair mismatches that may lead to alterations in the cellular faiths of the RNAs containing this modification. Parameters that are known to directly affect the stability of oligonucleotide structures, following the incorporation of oxidative lesions, include salt concentration (Na^+ ions), position of the lesion, and base pair identity amongst others.[19,20]

In this study, we describe the stabilization/destabilization effect that 8-oxoA has on homo- and hetero-duplexes of RNA:RNA and RNA:DNA structures, respectively, and on short hairpins of RNA. These structures are ubiquitous in nature and play essential roles in nature e.g., gene regulation, small molecule detection, and translation amongst many others. We found a direct relationship between the number of oxidative lesions in double stranded samples and an increased destabilization of these structures. However, the effects in short hairpins were position dependent with the stem being hypersensitive and the loop not affected. These differences are of importance, while increased destabilization may lead to faster degradation/disposal of the undesired oxidized RNA by endogenous processes, unchanged or increased stabilization may ensure the survival of the modified RNA and thus lead to deleterious effects e.g., errors in protein synthesis, changes in RNA reactivity.

RESULTS

We incorporated the oxidative lesion 8-oxoA into RNA via solid phase synthesis using its corresponding phosphoramidite.[21] The sequence chosen for the various RNA strands allowed us to study different secondary structures individually, i.e., duplex, heteroduplex, and hairpins. The stability changes that this lesion imparts on RNA:DNA double stranded samples were previously measured by Kim et al.[21] using 12-mers of RNA and displayed a depressed T_m of about 10.4°C (compared to its canonical analogue) when the modification was positioned opposite to thymidine (T). To explore the possible generalization of this result and learn more about this disruption in other assemblies, we decided to test the effect in stability of oligonucleotides containing 8-oxoA on 10-mers forming RNA:RNA homo- and RNA:DNA hetero-duplex structures. The length of these strands was chosen based on biologically relevant events that occur on RNA chains of similar dimensions such as the seed region in miRNA.[22,23] The duplex structures also contained base pair mismatches on both 5′- and 3′-ends to mimic some of the interactions observed between miRNA and mRNA structures. The sequence for the selected strands in this work (Figure 1) enabled us to test structures containing a single modification in different positions of the strand, that is, in the middle (single or consecutive modifications) or two bases away from the 3′-end using uridine (U/T) as its Watson-Crick complementary base pair. Melting temperatures were recorded by following the hypoellipticity of the CD band at $\lambda_{max} = 270$ nm.

We used circular dichroism as an indicator of the presence/absence of secondary structures. A single-stranded (ss) RNA displays a band with positive ellipticity at about 270 nm. This is in contrast with double stranded (ds-RNA) and/or formation of another structure containing an A-form duplex (i.e., hairpin, self-dimer, or pseudoknot), which can be characterized by (1) a hyperchromic shift in the band at 270 nm, and (2) the appearance of a band with negative ellipticity at about 210 nm. Also, a B-form duplex displays two main bands at about 280 and 240 nm with positive and negative ellipticity, respectively.

Consistent with this designation, CD spectra of single stranded RNA complement 6 showed a band with positive ellipticity ($\lambda_{max} = 270$ nm) only, indicating a lack of secondary

RNA*

5'-**UUG GXY GZC A**
UAC CUU CUG A-5'
or
TAC CTT CTG A-5'

RNA*	X	Y	Z
1	A	A	A
2	A	A	oxo-A
3	oxo-A	A	A
4	oxo-A	oxo-A	A
5	oxo-A	oxo-A	oxo-A

6 = 5' - AGU CUU CCA U

7 = 5' - AGT CTT CCA T

8 = 5' - TTG GAA GAC A

FIGURE 1 RNA sequence (left) of canonical and modified 10-mers hybridizing with their corresponding RNA or DNA complementary strands.

structure. On the other hand, spectra obtained from hybridization of canonical RNA 1 with RNA 6 or DNA 7, and of DNA 8 with DNA 7 showed the signature bands that indicate formation of their corresponding duplex structures (Figure 2). Solutions containing RNA 1:RNA 6 or RNA 1:DNA 7 assumed an A-form helix.[24] The observed band with negative ellipticity at about 240 nm has been assigned to the percent of single stranded regions.[25] Furthermore, increased ellipticity in a band with λ_{max} about 220 nm is consistent with an overall structure having features of both the B-form and A-form.[26] Control experiments to compare B-form DNA using the same sequence (DNA 7:DNA 8) displayed the expected spectrum.

CD spectra of RNA 1 alone showed bands [ellipticity at 270 (+), 240 (–), 220 (+), and 210 (–) nm] consistent with folding into a secondary structure. Attempts to obtain a T_m value failed and the lack of a defined sigmoidal curve suggested the presence of more than one structure.[27] Calculations[28] predicted formation of two hairpins, in agreement with the observed CD showing a secondary structure [Figure 2b and Table I, column 2]. Hybridization of RNA 1 with its corresponding complement six resulted in increased ellipticity of the CD bands observed in the absence of the complementary strand, in agreement with the formation of an A-form duplex. T_m measurements were recorded by following the hypoellipticity of the main band (λ_{max} = 270 nm), indicating dissociation of half of the ds-RNA population at 65.4°C (Table I, column 3). Double stranded heteroduplex and DNA:DNA samples were prepared in the same manner and displayed changes in their T_m of about 10.8 and 19.1°C lower, respectively.

Incorporation of one modification closer to the 3′-end yielded RNA 2, and as observed in strand 1, a secondary structure was observed in the absence of complement. T_m measurements showed a more defined transition, showing a clear sigmoidal shape, albeit with a T_m value lower than 10°C. This observation suggests for the presence of one structure that is stabilized by 8-oxoA, possibly folding to the hairpin containing a GAAGA* pentaloop (Figure 2b), where the modification at the first base in the loop provides stabilization of the structure *vide infra*. Subsequently, hybridization of RNA 2 with its RNA complement 6 resulted in duplex formation with a ΔT_m value

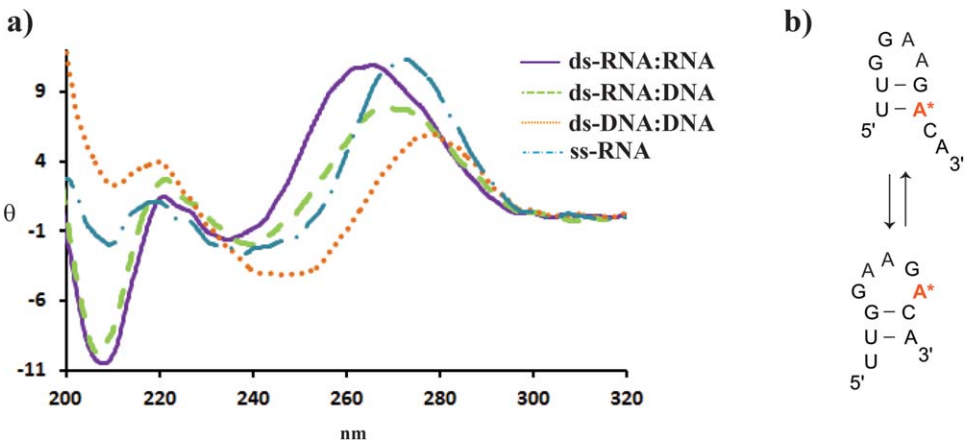

FIGURE 2 (a) CD spectra of canonical double stranded using strand 1, (ds) RNA:RNA, RNA:DNA, DNA:DNA, or RNA complement 6 as single stranded (ss) RNA structures. 25 μM RNA, 5 mM $MgCl_2$, 10 mM NaCl, and 1 mM sodium phosphate pH 7.2. (b) Predicted secondary structures obtained from RNAs 1 and 2.

Table I T_m Values of Homo- and Hetero-duplex of Canonical and Modified RNAs

		RNA:RNA	1 - Mod RNA	RNA:DNA	1 - Mod RNA	Homo–Hetero	Homo–Hetero
RNA	2° Structure (T_m)	T_m	ΔT_m	T_m	ΔT_m	ΔT_m	$\Delta\Delta T_m$
1	Yes (nd)	65.4 ± 0.3	–	54.6 ± 0.5	–	10.8 ± 0.7	–
2	Yes (< 10° C)	50.3 ± 0.1	15.1 ± 0.3	38.9 ± 0.3	15.7 ± 0.6	11.4 ± 0.3	− 0.6 ± 0.4
3	×	52.6 ± 0.8	12.8 ± 0.9	38.9 ± 0.1	15.7 ± 0.7	13.7 ± 0.9	− 2.9 ± 1.1
4	×	36.7 ± 0.7*	28.7 ± 0.8	24.3 ± 0.1*	30.3 ± 0.7	12.4 ± 0.7	− 1.6 ± 1.1
5	×	21.5 ± 0.4*	43.9 ± 0.5	< 10	> 35	na	na

T_m measurements of DNA 7:DNA 8 double stranded DNA yielded a value of 46.3 ± 0.2; ΔT_m = 19.0°C to RNA:RNA.
2° Structure indicates folding in the absence of complement.
ΔT_m (1 – Mod RNA) indicates the difference when compared to the canonical analogue.
ΔT_m (Homo–Hetero) indicates the difference in T_m between homo- and hetero-duplex structures.
$\Delta\Delta T_m$ represents the difference in ΔT_m between homo- and hetero-duplexes.
All T_m values were obtained via CD recorded at 270 nm.
The error represents that of experiments performed in duplicate* or triplicate.
nd, not determined; na, not applicable; Mod RNA, modified RNA structures 2–5.

about 15.1°C lower than its canonical analogue (Table I, column 4). This result shows that one 8-oxoA modification is sufficient to destabilize the double stranded structure significantly. Similarly, hybridization using DNA 7 yielded the corresponding RNA:DNA analogue and displayed a ΔT_m of about 15.7°C (Table I, column 6), thus indicating that the destabilization imposed by the lesion is similar to that obtained in the homoduplex structures.

To test for a position dependent effect, a single modification was incorporated in a region closer to the center of the strand to yield RNA 3. Although formation of a secondary structure was expected in the absence of complementary strands, CD did not display a band at 210 nm, thus indicating that the position of 8-oxoA in this region inhibits the folding observed on samples of both RNA strands 1 (canonical) and 2 (Figure 2b and Table I, column 2). We are investigating this observation further to address the effects of the lesion at this position (another unpredicted structure cannot be ruled out at the time). A decrease in stability was also detected upon formation of the corresponding RNA:RNA and RNA:DNA duplex with a ΔT_m of about −12.8 and −15.7°C with respect to one. This is in agreement with a larger disruption in the heteroduplex structures as the modification is further from the 3′-end. This may be due in part to a higher structural flexibility, thus suggesting for a lower impact in RNA:DNA complexes containing this lesion.

We then proceeded to test the effect of two consecutive modifications and synthesized RNA 4. In agreement with a larger number of oxidatively damaged nucleotides (one in the same position as in RNA 3), no secondary structure was observed in the absence of complementary strands (Table I, column 2). Furthermore, T_m measurements of hybridized samples showed a larger destabilization with respect to its canonical analogue one showing ΔT_m values of about 28.7 and 30.3°C in RNA:RNA and RNA:DNA, respectively. The difference with modified RNA 3 of about 15.9°C (in RNA:RNA) suggested the possibility of an additive effect as a function of number of lesions. To test this hypothesis we modified the canonical RNA at the three available sites to yield oligonucleotide five. T_m experiments performed on this RNA:RNA duplex showed a difference of 15.2°C with respect to RNA 4, well in agreement with the changes observed between RNAs 3 and 4. The same analysis could not be performed with the RNA:DNA heteroduplex due to the low T_m recorded (<10°C, Table I, column 5).

It is noteworthy that the difference between RNA:DNA duplexes three and four is also within the same range (14.6°C). This value is 4–5°C higher than that reported by Kim et al.,[21] presumably due to the higher G-C content present in the strands used in our work. We then used the change in molar ellipticity as a function of temperature to obtain thermodynamic parameters[29] on RNA:RNA duplexes formed with RNA strands 1, 3, 4, and 5 (see Supporting Information SI). Van't Hoff parameters, enthalpies (ΔH°), entropies (ΔS°), and free energies (ΔG°), were obtained from the slope and intercept of $1/T_m$ versus $\ln(C_T/4)$.[30] The change in free energy ($\Delta\Delta G^\circ$) from incorporation of one modification (RNA 1 compared to RNA 3) was of 0.9 Kcal/mol, while incorporation of two lesions resulted in a destabilization of about 2.7 Kcal/mol (RNA 1 compared to RNA 4). Attempts to obtain these parameters on RNA 5 yielded a poor R^2 value, presumably due to the low T_m value observed on this structure. These changes are

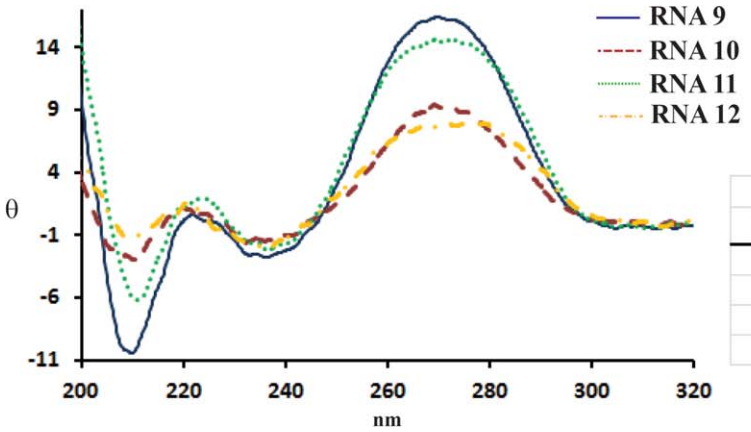

			Hairpin	9 - mod RNA
RNA	X	Y	T_m (°C)	ΔT_m
9	A	A	32.5 ± 1.0	—
10	oxo-A	A	< 10	> 22.5
11	A	oxo-A	33.1 ± 0.1	0.6 ± 1.0
12	oxo-A	oxo-A	nd	—

FIGURE 3 CD spectra (left) corresponding to the indicated RNA strands 9–12 (50 μM RNA, 5 mM $MgCl_2$, 10 mM NaCl, and 1 mM sodium phosphate-pH 7.2) and hairpin structure highlighting the modification sites (top right).

consistent with a decrease in duplex stability upon increasing the number of oxidative lesions within the duplex structures.

With the interest in testing the conformational changes imposed by this lesion on other structural motifs, we decided to use short hairpins with similar sequences to known RNA strands that met the following criteria: (1) T_m higher than room temperature, and (2) containing adenosine at both the stem and/or closing base pair of the loop. We chose a short hairpin composed of a three base pair long stem and a UUCA tetraloop (Figure 3). Hairpin formation was followed via CD and, as in the duplex structures, displayed bands with positive and negative ellipticities at about 270 and 210 nm, respectively. CD spectra of control oligonucleotide 9 displayed the expected bands characteristic of a hairpin structure, albeit with a lower T_m than that reported previously.[31] This difference can be rationalized with the fact that the authors used 5-methyluridine and other modifications within the stem. Melting temperatures for RNA strands 9–12 showed concentration independent profiles, in agreement with formation of the lowest energy structure mainly.[20] Substitution of A with 8-oxoA at the stem produced RNA 10, which resulted in significant destabilization that inhibited formation of the hairpin. This is evidenced in the CD spectra taken at room temperature and showing a single band with positive ellipticity, indicative of a single stranded structure ($\lambda_{max} = 270$ nm). Lowering the temperature (about 4°C) of samples containing 10 induced folding into a secondary structure (increased ellipticity and appearance of the band at 210 nm, Supporting Information SI), albeit at an incomplete stage, as observed via the lack of a sigmoidal curve upon melting. The observed ΔT_m of > about 22.5°C, with respect to its canonical analogue nine is larger than the difference of about 15°C observed on double stranded chains. This value however may vary with loop sequence and/or stem length, as the modification may stabilize/destabilize the overall structure.

As the stability of hairpins is known to be dependent on sequence and length, we set out to incorporate the oxidative lesion within the loop, one position from the closing base pair to yield RNA 11. As illustrated in Figure 3, CD spectra corresponding to RNA with substitution at A7 displayed bands consistent with formation of a hairpin and with no significant difference in ΔT_m values, which shows that modification at this position is not related to the stability of the hairpin. We then set out to test the possible formation of a hairpin upon concomitant modification at the two sites. RNA 12 was obtained and characterized as described below; however, CD spectra obtained at various temperatures (20–3°C) did not show formation of a secondary structure. These results indicate that both the position and the number of lesions may affect the overall structure in a different manner and magnitude.

To corroborate these observations and quantify the effect of 8-oxoA within the stem, we decided to increase the length of the stem by adding a C-G base pair without varying the sequence of the tetraloop. The design was such that similar positions to those in the shorter hairpins were also modified, leading to RNAs 13–16 (Figure 4). As indicated in Table II and in agreement with a longer stem, we found that melting of the canonical hairpin 13 occurred with a difference of about +27.6°C with respect to its shorter analogue (10-mer). Incorporation of 8-oxoA at the stem yielded RNA 14, which displayed a CD pattern consistent with formation of a hairpin and resulted in a T_m depression of about 24.9°C. As in the case of the shorter analogue 10, this value is in agreement with a larger destabilization than that observed in the duplex samples.

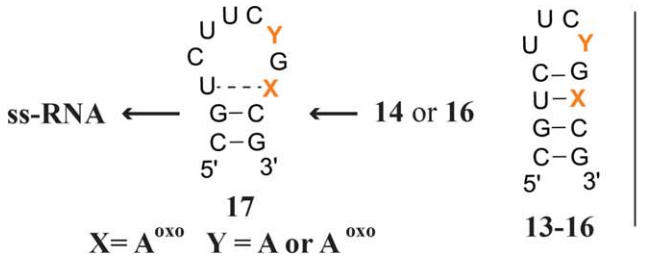

RNA	X	Y	Hairpin T_m (°C)	13 - mod RNA ΔT_m
13	A	A	60.1 ± 0.5	—
14	oxo-A	A	35.2 ± 0.2	24.9 ± 0.5
15	A	oxo-A	60.7 ± 0.5	0.6 ± 0.8
16	oxo-A	oxo-A	40.1 ± 0.6*	20.0 ± 0.8

FIGURE 4 (right) and Table II (left). Hairpin sequence and structure of RNA strands 13–16 containing tetraloop UUCX (X = A or 8-oxoA) and its proposed transformation from 14/16 to 17 (left). T_m and ΔT_m values of RNAs 13–16. All T_m values were obtained via CD at 270 nm. Experiments were performed in triplicate or duplicate* (right). Mod RNA = modified RNA structures 14–16.

We also reasoned that this observation may be attributed to the proximity of the modification to the loop, thus setting up formation of a less stable structure (RNA 17) containing a larger loop (UCUUCAGA^{oxo})/shorter stem (G:C, C:G) or hexaloop (CUUCAG)/stem (U:A^{oxo}, G:C, and C:G). To validate the formation of a hairpin with a larger loop, we synthesized two RNA models designed to form an octaloop or a hexaloop. (Figure 4). Strands 18 and 19 displayed CD spectra consistent with hairpin formation and showed T_m values of 18.1 and 44.5°C. These results are in agreement with structural transformation 14 → 17, with a T_m value that shows preference for formation of a hairpin containing a hexaloop and not an octaloop (RNA 17).

To test for the effect upon modification at the loop, we synthesized RNA 15. As in the case of the shorter hairpin, T_m measurements displayed a value that is within error of its canonical analogue 10 (T_m = 60.7°C) showing no obvious interactions at this position. As a last control, we synthesized disubstituted RNA strand 16. Contrary to the results obtained for the shorter hairpin 12, RNA 16 showed formation of a hairpin with a measurable melting temperature about 4.9°C higher than that of oligonucleotide 14 (containing a single modification at the stem). This observation suggests formation of a more stable hairpin structure upon concomitant modification of the stem and loop regions, consistent with the proposed formation of RNA 17 (hexaloop). It is known for the identity of this position to be in direct relationship with both the stem and the loop, and thus impact the stability of the hairpin.[32,33] One explanation can be found in the possible increased stacking interaction between 8-oxoA and G_8,[34] which may arise from the feasibility of 8-oxoA to exist in either syn- or anti-conformations.

DISCUSSION

To test the implications regarding the stability and structural changes imposed by 7,8-dihydro-8-oxoadenosine (8-oxoA) on oligonucleotides of RNA forming different secondary structures, we incorporated 8-oxoA into specific sites of RNA. CD confirmed formation of the targeted secondary structures, i.e., double stranded DNA:RNA/RNA:RNA and short hairpins. We found that incorporation of a single lesion destabilized both RNA:RNA and RNA:DNA duplex structures, reflected by a T_m depression of as much as about 15.7°C. The position of the modification did not have an effect on the heteroduplex, however, RNA:RNA double stranded samples experienced a larger disruption (about 2.4°C) when the lesion was closer to the 3′-end (RNA 2). These results are in agreement with the destabilization trend observed by Kim et al.[21] on 12-mers of an RNA:DNA duplex containing a single lesion. In addition, we found that incorporation of two or three modifications led to detrimental ΔT_m values between 13 and 16°C each, thus suggesting that this may be a reasonable temperature range to predict the effect of this modification in oligonucleotides of RNA. We also confirmed the known stability trend on canonical homo- and hetero-duplexes (RNA:RNA > RNA:DNA > DNA:DNA),[35,36] and found that the effect of the modification on homo- or hetero-duplexes is independent of structure.

8-oxoA was incorporated on 10-mers and 12-mers of RNA that folded into short hairpins containing a UUCX (X = A, 8-oxoA) tetraloop. The stem was lengthened from three (RNA 9–12) to four (RNA 13–16) base pairs as a way to increase the melting transitions and quantify some of the effects not

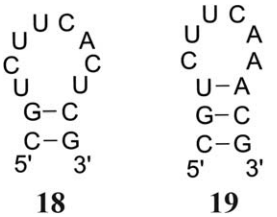

RNA	Hairpin T_m (°C)
18	18.1 ± 0.6
19	44.5 ± 0.1

FIGURE 5 Sequence and structure of RNA strands 18 and 19. T_m values were obtained from their CD spectra and were performed in triplicate.

observed in the shorter series. CD spectra corresponding to both canonical RNA strands 9 and 13 folded into the expected hairpin displaying melts at about 32.5 and 60.1°C. We then introduced a modification at the stem of both hairpins to obtain RNAs 10 and 14, and found that 8-oxoA inhibited formation of the secondary structure in the shorter stem (cooling the sample to 4°C induced hairpin formation, $T_m < 10$°C). On the other hand, oligonucleotide 14 and 16 folded into a secondary structure that displayed a larger destabilization (T_m lower by about 25 and 20°C from control) than that observed on the duplex samples. We concluded that both RNA strands 14 and 16 are likely to form a structure resembling that of RNA 17 (hexaloop), with T_m values falling closer to hexaloop hairpin model 19 than octaloop hairpin 18.

Modification of the loop region in the presence/absence of a modified stem (RNAs 11 and 15) resulted in no effect toward the secondary structure, as evidenced by the similarity in T_m values (within error). These results are in agreement with the proposed structures for ss-RNA-1 and ss-RNA-2 (Figure 2, right), in which the presence of 8-oxoA stabilizes one structure over the more stable hairpin. Another example of this effect is observed in the formation RNA 17, where the presence of this oxidative lesion leads to a different structure that is stable at room temperature. Finally, concomitant substitution at the stem and loop in RNA 12 inhibited folding into a secondary structure, while longer RNA 16 formed a hairpin, which showed to be more stable than its stem-substituted analogue 14 (about +4.9°C difference). This result may be explained through the formation of another structure such as RNA 17 or via the synergy of two effects, destabilization at the stem with stabilization at the loop.

Overall, we found that the effect of the oxidative lesion 8-oxoA in oligonucleotides of RNA can be position dependent and while a destabilizing effect is generally expected in double stranded regions of RNA:RNA or RNA:DNA duplex structures, it may also give rise to other structural motifs. These results are of importance, as the functionality within structurally dependent RNA may be altered upon oxidative stress in biologically relevant systems. While the destabilization observed in the presence of two or more lesions may be desired to promote degradation of the modified RNA, modification at other positions such as the loop in a hairpin may have no effect. In this case, the consequences regarding the presence of the lesion may result in deleterious effects due to the retention of secondary structure with modified RNAs. We are in the process of expanding this study to other more structurally complex structures to explore the generality of the results presented in this study. We are also interested in incorporating this lesion into functional RNAs e.g., miRNAs and siRNAs,[37,38] to explore the outcomes inflicted by this lesion on biologically relevant processes.

CONCLUSION

We incorporated the oxidative lesion 7,8-dihydro-8-hydroxyadenosine into oligonucleotides of RNA and used circular dichroism to asses structure and stability changes imposed by this modification. Short hairpins, homo-, and heteroduplexes were used as models. We found that the effects of this lesion depend on position and number of modifications and may result in altered stability. Although destabilization can be generally expected, there are instances in which stabilization may occur and lead to the formation of other structural motifs. We are currently exploring the relationship between the effects of this lesion and RNA function using other systems.

EXPERIMENTAL SECTION

General Methods

Mass spectra (MALDI-TOF MS) were recorded on an ABI 4800 Plus MALDI TOF/TOF analyzer. Melting points were obtained using a DigiMelt MSRS. CD spectra were recorded using a J-815 circular dichroism spectropolarimeter. Samples for MALDI-TOF analysis were prepared according to a previous procedure using a 2,4,6-trihydroxyacetophenone (THAP).[39] Oligonucleotides were synthesized on an applied biosystems incorporated 394 oligonucleotide synthesizer. Oligonucleotide synthesis reagents were purchased from Glen research (Sterling, VA) and used without further purification.

CD Spectroscopy

CD spectra were recorded on a Jasco-815 spectropolarimeter at various temperatures (PTC-348W1 peltier thermostat) using Quartz cuvettes with a 0.1 cm path length. Spectra were averaged over three scans (330–190 nm, 0.5 nm intervals, 1 nm bandwidth, and 1 s response time) and background corrected with the appropriate buffer or solvent. Solutions containing the RNA strands 9–12 had the following composition: 50 μM RNA, 5 mM $MgCl_2$, 10 mM NaCl, and 1 mM sodium phosphate-pH 7.2. All others contained 25 μM in RNA/DNA using the same buffer and salinity. All solutions were hybridized before recording spectra by heating to 90°C followed by slow cooling to room temperature. Melting temperatures were recorded at 270 nm with a ramp of 1°/min and step size of 0.2 and were determined from the maximum in the first derivative of the melting curve.

SUPPORTING INFORMATION

MS spectra corresponding to the characterization of the described RNAs is included. CD spectra of all the pertinent

experiments, including melting temperature measurements can also be found therein. Van't Hoff plots and thermodynamic parameters is included along with NMR, IR, and HRMS data corresponding to the characterization of the phosphoramidite of 8-oxoA.

Yu Jung Choi acknowledges a UROP award from CU Denver for support. CD was performed at the Biophysics core facilities, Structural Biology and Biochemistry, University of Colorado, Anschutz Medical Campus. Mass spectrometry of oligonucleotides was performed at the Mass spectrometry core facilities, University of Colorado, Skaggs School of Pharmacy and Pharmaceutical Sciences, Anschutz Medical Campus.

REFERENCES

1. Dickinson, B. C.; Chang, C. J. Nat Chem Biol 2011, 7, 504–511.
2. Fleming, A. M.; Muller, J. G.; Dlouhy, A. C.; Burrows, C. J. J Am Chem Soc 2012, 134, 15091–15102.
3. Zhou, C.; Greenberg, M. M. J Am Chem Soc 2014, 136, 6562–6565.
4. Bohne, C.; Faulhaber, K.; Giese, B.; Häfner, A.; Hofmann, A.; Ihmels, H.; Köhler, A. -K.; Perä, S.; Schneider, F.; Sheepwash, M. A. L. J Am Chem Soc 2005, 127, 76–85.
5. Cadet, J.; Douki, T.; Gasparutto, D.; Ravanat, J. L. Mutat Res 2003, 531, 5–23.
6. Poulsen, H. E.; Specht, E.; Broedbaek, K.; Henriksen, T.; Ellervik, C.; Mandrup-Poulsen, T.; Tonnesen, M.; Nielsen, P. E.; Andersen, H. U.; Weimann, A. Free Radical Bio Med 2012, 52, 1353–1361.
7. Cooke, M. S.; Evans, M. D.; Dizdaroglu, M.; Lunec, J. FASEB J 2003, 17, 1195–1214.
8. De Bont, R.; van Larebeke, N. Mutagenesis 2004, 19, 169–185.
9. Henriksen, T.; Hillestrøm, P. R.; Poulsen, H. E.; Weimann, A. Free Radical Bio Med 2009, 47, 629–635.
10. Nunomura, A.; Moreira, P. I.; Takeda, A.; Smith, M. A.; Perry, G. Curr Med Chem 2007, 14, 2968–2975.
11. Li, Z.; Wu, J.; Deleo, C. J. IUBMB Life 2006, 58, 581–588.
12. Steenken, S.; Jovanovic, S. V. J Am Chem Soc 1997, 119, 617–618.
13. Singh, T. A.; Rao, B. S. M.; O'Neill, P. J Phys Chem B 2010, 114, 16611–16617.
14. Rokhlenko, Y.; Geacintov, N. E.; Shafirovich, V. J Am Chem Soc 2012, 134, 4955–4962.
15. Nilov, C. I.; Komarov, D. Y.; Panov, M. S.; Karabaeva, K. E.; Mereshchenko, A. S.; Tarnovsky, A. N.; Wilson, R. M. J Am Chem Soc 2013, 135, 3423–3438.
16. von Sonntag, C. Free-Radical-Induced DNA Damage and Its Repair; Springer-Verlag: Berlin, 2006; pp 371–377.
17. Barone, F.; Cellai, L.; Giordano, C.; La Sala, G.; Mazzei, F. Int J Radiat Biol 2002, 78, 9–16.
18. Yanagawa, H.; Ogawa, Y.; Ueno, M. J Biol Chem 1992, 267, 13320–13326.
19. Singh, S. K.; Szulik, M. W.; Ganguly, M.; Khutsishvili, I.; Stone, M. P.; Marky, L. A.; Gold, B. Nucleic Acids Res 2011, 39, 6789–6801.
20. Meroueh, M.; Chow, C. S. Nucleic Acids Res 1999, 27, 1118–1125.
21. Kim, S.; Kim, J. Y.; Baek, A. K.; Moon, B. J. Bioorg Med Chem Lett 2002, 12, 1977–1980.
22. MacFarlane, L. -A.; Murphy, P. R. Curr Genomics 2010, 11, 537–561.
23. Ameres, S. L.; Zamore, P. D. Nat Rev Mol Cell Bio 2013, 14, 475–488.
24. Ranjbar, B.; Gill, P. Chem Biol Drug Des 2009, 74, 101–120.
25. Newbury, S. F.; McClellan, J. A.; Rodger, A. Anal Commun 1996, 33, 117–122.
26. Kim, S. K.; Lee, S. H.; Kwon, O. S.; Moon, B. J. J Biochem Mol Biol 2004, 37, 657–662.
27. Gao, Y.; Wolf, L. K.; Georgiadis, R. M. Nucleic Acids Res 2006, 34, 3370–3377.
28. Markham, N. R.; Zuker, M. In Bioinformatics, Vol. II. Structure, Functions, and Applications, number 453 in Methods in Molecular Biology; Keith, J. M., Ed.; Humana Press: Totowa, NJ, 2008; Chapter 1, pp 3–31.
29. Mikulecky, P. J.; Feig, A. L. Biopolymers 2006, 82, 38–58.
30. Aboul-ela, F.; Koh, D.; Tinoco, I., Jr. Nucleic Acids Res 1985, 13, 4811–4824.
31. Resendiz, M. J. E.; Schön, A.; Freire, E.; Greenberg, M. M. J Am Chem Soc 2012, 134, 12478–12481.
32. Deng, N. -J.; Cieplak, P. Biophys J 2010, 98, 627–636.
33. Ma, H.; Proctor, D. J.; Kierzek, E.; Kierzek, R.; Bevilacqua, P. C.; Gruebele, M. J Am Chem Soc 2006, 128, 1523–1530.
34. Williams, D. J.; Hall, K. B. J Mol Biol 2000, 297, 1045–1061.
35. Clark, C. L.; Cecil, P. K.; Singh, D.; Gray, D. M. Nucleic Acids Res 1997, 25, 4098–4105.
36. Cheatham, T. E., III; Kollman, P. A. J Am Chem Soc 1997, 119, 4805–4825.
37. Ghanty, U.; Fostvedt, E.; Valenzuela, R.; Beal, P. A.; Burrows, C. J. J Am Chem Soc 2012, 134, 17643–17652.
38. Hernández, A. R.; Peterson, L. W.; Kool, E. T. ACS Chem Biol 2012, 7, 1454–1461.
39. Chapman, E. G.; DeRose, V. J. J Am Chem Soc 2010, 132, 1946–1952.

Reviewing Editor: Nils G. Walter